SCIENTIFIC REPORTS

OPEN

SUBJECT AREAS:
EXPERIMENTAL MODELS OF DISEASE
CANCER MICROENVIRONMENT
METASTASES
TRANSLATIONAL RESEARCH

Received
19 March 2013

Accepted
16 July 2013

Published
9 August 2013

The brain microenvironment negatively regulates miRNA-768-3p to promote *K-ras* expression and lung cancer metastasis

Arasukumar Subramani[1,2]*, Samer Alsidawi[1,2]*, Sajjeev Jagannathan[1,2], Kazutaka Sumita[1,2], Atsuo T. Sasaki[1,2], Bruce Aronow[3], Ronald E. Warnick[1,4,5], Sean Lawler[6] & James J. Driscoll[1,2]

[1]Division of Hematology and Oncology, University of Cincinnati College of Medicine, Cincinnati, OH 45267-0508, USA, [2]The Vontz Center for Molecular Studies, Department of Internal Medicine, University of Cincinnati College of Medicine, Cincinnati, OH 45267-0508, Cincinnati, OH 45267-0508, USA, [3]Cincinnati Children's Hospital Medical Center, Division of Biomedical Informatics, Cincinnati, OH 45229-3026, USA, [4]Department of Neurosurgery, University of Cincinnati College of Medicine, Cincinnati, OH 45267-0508, USA, [5]The Brain Tumor Center at the University of Cincinnati Neuroscience Institute, Cincinnati, OH 45267-0508, USA, [6]Leeds Institute of Molecular Medicine, University of Leeds, UK.

Correspondence and requests for materials should be addressed to J.J.D. (driscojs@uc.edu)

* These authors contributed equally to this work.

The brain microenvironment promotes metastasis through mechanisms that remain elusive. Co-culture of lung cancer cells with astrocytes - the most abundant cell type within the metastatic brain niche – lead to downregulation of miRNA-768-3p which drives *K-ras* expression and key signaling pathways, enhances cell viability and promotes chemotherapeutic resistance. Vector-based forced expression of miRNA-768-3p complementary sequence or a chemically-engineered miRNA-768-3p inhibitor recapitulated the astrocyte effect to increase tumor cell viability. The miRNA-768-3p inhibitor targeted the *K-ras* 3′-UTR as demonstrated by increased luminescence from a luciferase reporter and strikingly increased the K-ras protein and the downstream effectors ERK1/2 and B-Raf. miRNA-768-3p was reduced in patient brain metastases compared to normal brain tissue and was lower in patient tissue from brain metastases compared to same-patient primary tumour tissue. The brain microenvironment negatively regulates miRNA-768-3p to enhance *K-ras* and promote metastasis. We propose that therapeutic replacement of the metastasis suppressor miRNA-768-3p holds clinical promise.

Over 170,000 patients are annually diagnosed in the United States with metastatic brain lesions - ten times the incidence of primary brain tumours[1,2]. Brain metastases remain a challenging complication in the treatment of systemic cancers despite surgical advances and the advent of targeted therapies[3]. Most deaths due to cancer result from the progressive growth of metastatic, drug-resistant lesions[1–3]. Moreover, the incidence of brain metastases is rising as a result of superior imaging modalities, methods for earlier detection of cancers and more effective treatments for systemic disease[3]. Median survival for untreated patients with metastatic brain lesions is ~ 2 months, which can extended to 12–15 months with radiosurgery and chemotherapy[4]. Additional consequences include a negative impact on cognition, memory, language and mobility which take their toll on patients, families and the healthcare system[4,5].

The resistance of tumour cells growing in the brain parenchyma to chemotherapy has been attributed to the inability of circulating chemotherapeutic drugs to penetrate the blood-brain barrier (BBB), which is composed of brain endothelial cells with tight junctions enwrapped with basement membrane, pericytes and astrocytes[6]. However, tumour cells within the brain parenchyma release vascular endothelial growth factor and other cytokines that increase vessel permeability. Together with clinical observations that brain metastases are diagnosed as lesions surrounded by edema and that exhibit leakiness of contrast material, these findings rule out the BBB as a sole mechanism of drug resistance[7]. Alternatively, overexpression of P-glycoprotein, a membrane protein that expels drugs from a cell's cytoplasm, by tumour cells growing in the brain microenvironment has also been implicated in tumour cell resistance to chemotherapy[8]. Clinical trials using inhibitors of P-glycoprotein, however, failed to reverse the resistance of tumour cells to chemotherapeutic drugs or increase the response rate.

Collectively, these studies indicate that unidentified mechanisms underlie the pro-survival effect of the brain microenvironment.

MicroRNAs (miRNAs) are attractive candidates as upstream regulators of metastatic progression since a single miRNA can post-transcriptionally regulate entire sets of genes[9–13] and recent studies have revealed a critical role for miRNAs during tumourigenesis and metastasis[14,15]. Metastases develop when tumour cells usurp homeostatic mechanisms and exploit the cytoprotective properties of astrocytes. However, the molecular networks necessary to establish brain metastases remain obscure. Histologic examination of clinical specimens from human brain metastases and experimental murine brain metastases has revealed that they are surrounded by reactivated astrocytes, the most common cell type in the brain. Metastatic lesions surrounded by activated astrocytes are highly resistant to chemotherapy[16–18]. The potential role of astrocytes in the regulation of brain metastasis through altered tumour miRNA expression has not yet been addressed. Here we demonstrate that astrocytes co-culture modulates the level of miRNAs in lung cancer cells. Specifically, reduction in the level of miRNA-768-3p or engineered-inhibition of miRNA-768-3p leads to increased cell viability by targeting of *K-ras*. Finally, miRNA-768-3p levels are reduced in patient tumour metastasis samples, supporting its role in the establishment of brain metastases in cancer progression.

Results

Astrocyte co-culture. The majority of brain metastases originate from one of three primary malignancies: lung cancer (40%–50%), breast cancer (15%–25%), or melanoma (5%–20%)[4,5]. To investigate the pro-survival effect of the brain microenvironment, lung, breast and melanoma cells were co-cultured with conditionally immortal astrocytes from a line derived from *H-2Kb-tsA58* mice[19]. Prior studies demonstrated that astrocytes activate programs in lung adenocarcinoma cells (PC14-PE6) to support cell division and survival[19]. Co-culture with astrocytes enhanced cell viability and proliferation compared to growth alone or after co-culture with control 3T3 fibroblasts (Fig. 1A, B). Astrocytes also promoted a pro-survival, chemo-protective effect on tumour cells as shown by enhanced resistance to multiple cytotoxic agents (Fig. 1C). The cytoprotective effect was optimal when the astrocytes were in direct contact with the tumour cells and the effect was blocked by the gap junction inhibitor carbenoxolone (CBX) (Fig. 1D, E). Spherical, heterogeneous aggregates of proliferating, quiescent, and necrotic cells in culture retain three-dimensional architecture and tissue-specific functions. Since the ability to form spheroids is a characteristic trait of cultured cells derived from solid tumours, we addressed the effect of the immortalized murine astrocytes on these properties. H520 (lung) and MCF7 (breast) cells were co-cultured with immortalized astrocytes and sphere-formation measured. Astrocyte co-culture increased the number of spheroid-like structures in tumour cell cultures (Fig. 1F) and also increased invasion (Fig. 1G).

MiRNA profiling of tumour cells after astrocyte co-culture. MiRNAs are small non-coding RNA molecules that regulate gene expression, influence tumour cell growth and contribute to metastasis. To address the role of miRNAs in astrocyte-induced tumour growth, global microarray-based analysis was performed to profile miRNA expression in tumour cells before and after astrocyte co-culture using. H520 and MCF-7 cells were grown either alone, with GFP^+-3T3 fibroblasts or with GFP^+-astrocytes (Supp. Fig. 1). After co-culture, tumour cells were separated from the adherent GFP^+-murine astrocytes, total mRNA isolated and miRNAs identified that were significantly altered in the tumour cells. We focused on those miRNAs that were reduced after co-culture since such changes could eventually be corrected through replacement with chemical-engineered mimics. Heat maps compared the fold-reduction in the level of individual miRNAs in tumour cells after co-culture with astrocytes (Fig. 2A). Analysis indicated that miRNA-768-5p was significantly reduced (8-fold) in breast tumour cells while an alternatively processed variant miRNA-768-3p was reduced 4-fold in lung tumour cells (Supp. Fig. 3). A comparison of previously published box C/D snoRNA and miRNA sequences and public databases revealed that the previously described miRNAs miR-768-3p and miR-768-5p both are located within the sequence of the snoRNA HBII-239[20,21]. Subsequently, it was found that HBII-239 produces a ~ 30 base-long RNA fragment which includes the reported miR768-3p sequence. HBII-239, the precursor for miR-768-3p and miR-768-5p, corresponds to a putative box C/D snoRNA, whose existence was predicted by homology to the experimentally identified mouse snoRNA MBII-239. HBII-239 has only recently been detected in human cells and is a fibrillarin-associated snoRNA[22]. As discussed below, chemically-synthesized mimics and inhibitors were generated to investigate the functional role of miR-768-3p and miR-768-5p as opposed to a potential effect of the precursor snoRNA HB-239.

Other miRNAs significantly decreased in either lung tumour or breast tumour cells after co-culture with astrocytes (but not 3T3 cells) were detected (Supp. Tables 1, 2; Supp. Fig. 2). Importantly, the miRNAs reduced in tumour cells were detected at much higher levels in fibroblasts or astrocytes alone indicating that the reduction detected in the tumour cells was not due to cross-contamination by other cell types. In addition, the microarray probes used for our analysis were specifically designed to detect human miRNAs to reduce the effect of any murine astrocyte derived contaminating miRNA. Astrocyte co-culture reduced miRNA-768-3p in lung tumour cells not only by fold-reduction (Fig. 2A) but also by reduction in absolute expression level (Fig. 2B). To support the microarray results, lung or breast tumour cells were co-cultured with astrocytes and led to a significant decrease in miRNA-768-3p by RT-PCR (Fig. 2C). MiRNAs-886-5p and 200c were strongly downregulated in co-cultured tumour cells (Supp. Fig. 3). Prior studies demonstrated that miRNA-886-5p inhibits apoptosis by down-regulating *Bax* in cervival carcinoma cells[23] and that miRNA-200c modulates the stem cell self-renewal regulator BMI1 and may inhibit clonal expansion of breast cancer cells[24]. We focused on miRNA-768-3p since it was significantly reduced in both tumour cell types after co-culture and its role in cancer and metastasis has not yet been studied.

Inhibition of individual miRNAs recapitulates the pro-survival astrocyte effect. Forced expression of sequence complementary to endogenous miRNAs, known as antagomirs, has been shown to efficiently bind to target gene 3′-untranslated regions (UTRs) and disrupt miRNA-mediated target gene regulation[34]. To examine the role of miRNA-768 in tumour cell functions, sequences complementary to miRNA-768-3p or 768-5p were designed and cloned into the pEZ-AMO1 expression vector. A control vector that expressed scrambled sequence or vectors that expressed either miRNA-768-3p or miRNA-768-5p antagomirs were transfected into tumour cells and the effect on cell viability determined (Fig. 3A). The miRNA-768-3p antagomir enhanced cell viability in both lung and breast tumour cells.

Chemically-engineered miRNA-768-3p inhibitor effect on cell growth and drug resistance. Since vector-based expression of the miRNA-768-3p antagomir enhanced cell growth, chemically-engineered inhibitors were designed based upon the sequence of miRNAs that were reduced in the lung tumour cells after astrocyte co-culture. The miRNA inhibitors were designed as complementary sequence, similar to the antagomirs, to silence specific individual, endogenous miRNAs. Transfection of a miRNA-768-3p inhibitor into A549 cells increased viability in a dose-dependent manner compared to cells transfected with the scrambled control (Fig. 3B). A panel of chemically-engineered inhibitors directed against other

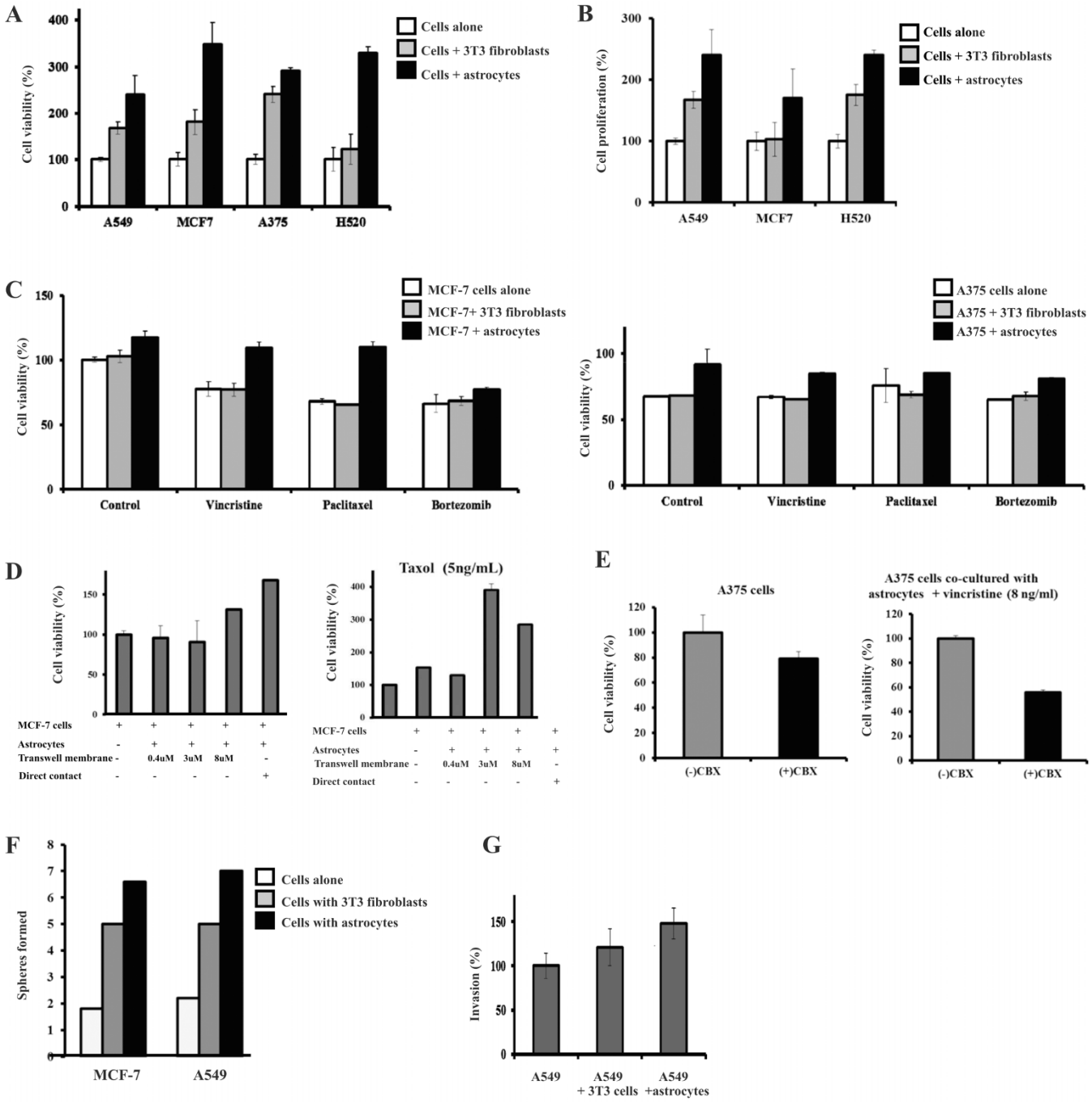

Figure 1 | Pro-survival effects of astrocytes on solid tumour cells. (A). Astrocyte effect on tumour cell viability was determined using the XTT assay. The average of triplicate measurements is shown and error bars represent the standard deviations. (B). Astrocyte effect on tumour cell proliferation was determined using bromodeoxyuridine (BrDU) assay. The average of triplicate measurements is shown and error bars represent the standard deviations. (C). Effect of astrocytes on viability of H520 lung, MCF-7 breast and A375 melanoma cells after treatment with vincristine, paclitaxel or bortezomib. Tumour cells were cultured alone, with 3T3 cells or astrocytes. Tumour cells were removed, treated with drugs at indicated concentrations and viability determined by the XTT assay. The average of triplicate measurements is shown and error bars represent the standard deviations. (D). Effect of transwell pore size or direct contact on astrocyte-mediated growth effect on tumour cells. Tumour cells were cultured either alone, co-cultured with astrocytes separated by transwell inserts with indicated membrane pore sizes or in direct contact with the astrocytes. Tumour cells were then removed and used viability determined by the XTT assay. The average of triplicate measurements is shown and error bars represent the standard deviations. (E). Effect of the gap junction inhibitor carbenoxolone (CBX) on the astrocyte-mediated growth effect. The effect of CBX alone on A375 cells was determined by XTT assay. A375 cells were also co-cultured with astrocytes in the presence or absence of CBX and the effect of vincristine on cell viability then determined. (F). Effect of astrocytes on tumour cells to form spheres. MCF-7 and A549 cells were co-cultured with astrocytes and the ability to form spheres determined by counting the number of spheres in each quadrant of the flask counted. Shown is the average value from the 4 quadrants for each cell line alone, with 3T3 fibroblasts or astrocytes. (G). Effect of astrocytes on tumour cell invasion. Tumour cells were cultured either alone, with 3T3 fibroblasts or astrocytes in BioCoat™ BD Matrigel™ invasion chambers with 8.0 μm polyethylene terephthalate membrane 6-well cell culture inserts (Becton-Dickson, Franklin Lakes, NJ).

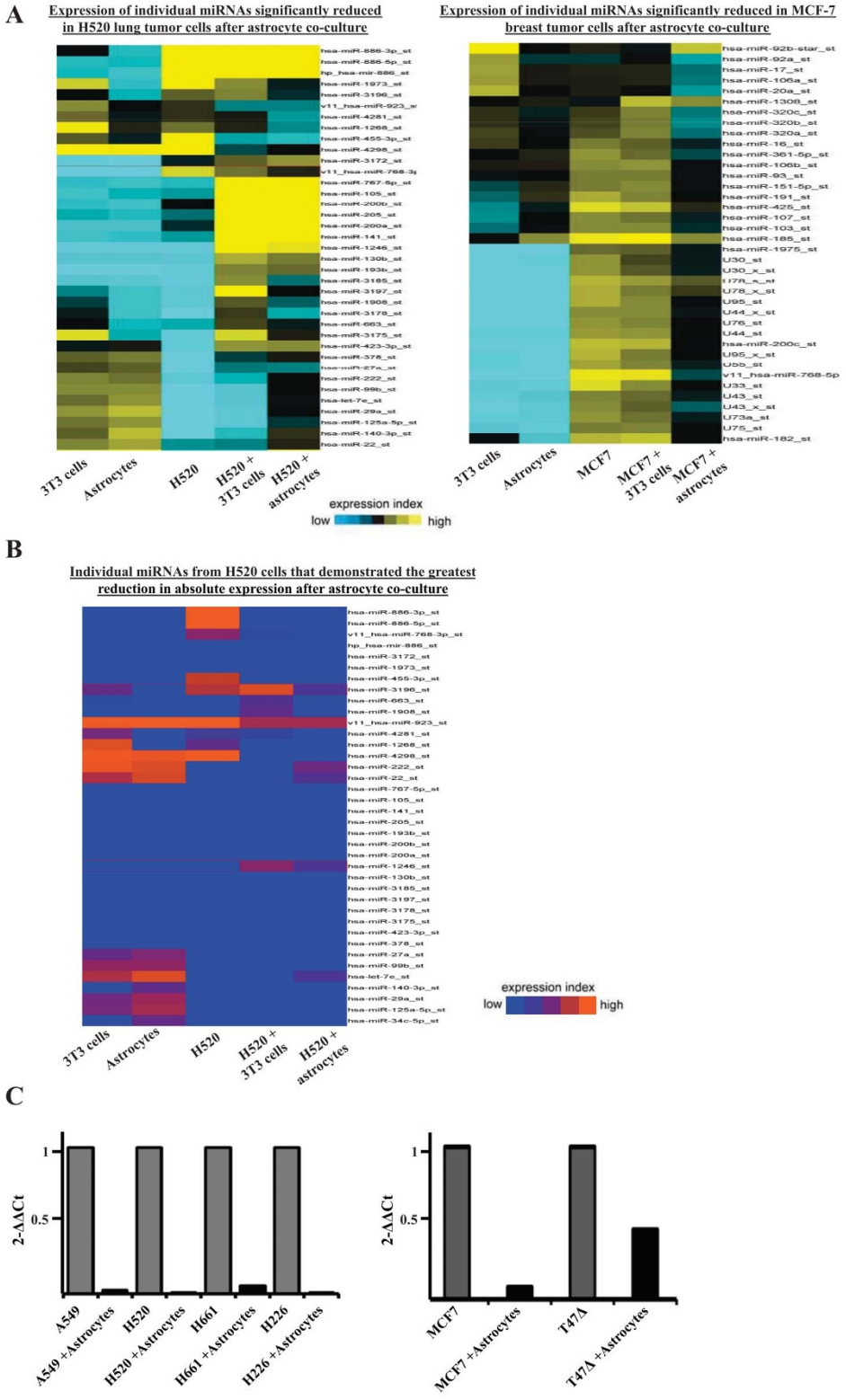

Figure 2 | miRNAs reduced in H520 lung and MCF-7 breast tumour cells after astrocyte co-culture. (A). H520 lung or MCF-7 breast tumour cells were grown either alone or co-cultured with 3T3 fibroblasts or astrocytes for 48 h. Tumour cells were then removed, washed in PBS and total RNA was isolated from the 3T3 fibroblasts, murine astrocytes, MCF-7 cells, H520 cells and tumour cells that had been co-cultured with either 3T3 cells or astrocytes. The level of individual miRNAs in each sample was then determined using Affymetrix microarrays. Shown are individual miRNAs that were significantly reduced in tumour cells after astrocyte co-culture by fold-reduction compared to their expression level in untreated tumour cells. Also shown is the relative level of expression of each miRNA in either the 3T3 fibroblasts, astrocytes or tumour cells alone. (B). Individual miRNAs from H520 cells that demonstrated the greatest reduction in absolute expression after astrocyte co-culture. Shown are miRNAs from H520 cells that displayed the greatest reduction in absolute expression after comparing the level in untreated cells to those co-cultured with astrocytes. (C). Effect of astrocyte co-culture on the relative expression of miRNA-768-3p in lung and breast tumour cells. RT-PCR quantitated the level of miRNA-768-3p in tumour cells after 72 h co-culture with astrocytes.

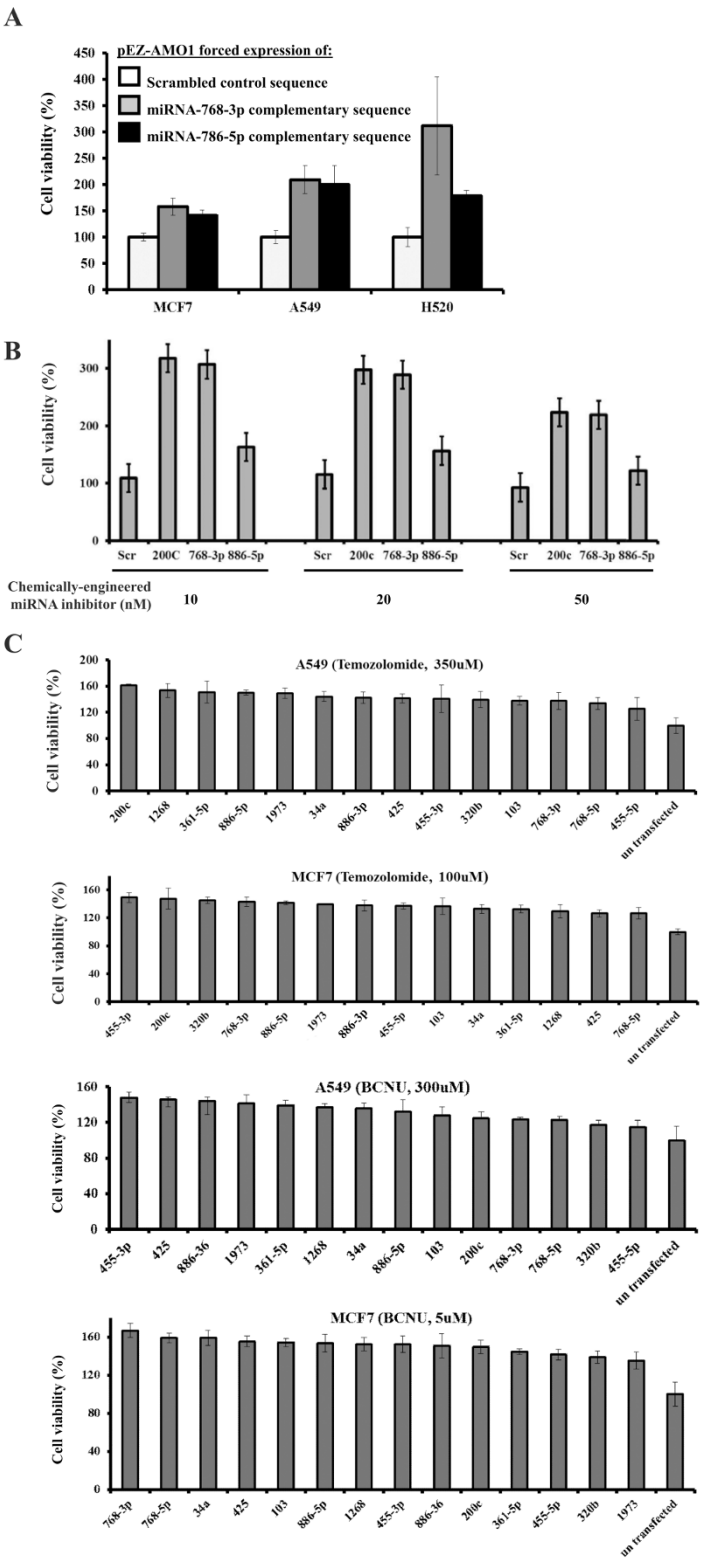

Figure 3 | Effect of forced expression of complementary sequence and a chemically-synthesized miRNA-768-3p inhibitor on viability. (A). Effect of vector-based forced expression of sequences complementary to miRNA-768-3p and 768-5p or scrambled sequence (control) on MCF-7, A549 and H520 tumour cell viability. The average of triplicate measurements is shown and error bars represent the standard deviations. (B). Dose-dependent effect of chemically-engineered miRNA inhibitors on cell viability. Chemically-engineered miRNA oligonucleotide sequences complementary to and designed to inhibit individual miRNAs or a scrambled sequence (control) were transfected into tumour cells at indicated concentrations. After growth for 48 h, cells were removed and viability determined by the XTT assay. Shown is the average of triplicate measurements. The average of triplicate measurements is shown and error bars represent the standard deviations. (C). Effect of chemically-engineered miRNA inhibitors on cell viability in the presence of TMZ or BCNU. Cells were transfected with individual chemical inhibitors to the respective miRNAs, allowed to incubate for 48 h and then plated in 96-well plates. Cells were then grown in the absence or presence of temozolomide or carmustine (BCNU) for 72 h, cell viability determined using the XTT assay. The average of triplicate measurements is shown and error bars represent the standard deviations.

miRNAs reduced by co-culture was used to address their effect on the growth of tumour cells in the presence of chemotherapeutic agents. We chose temozolomide (TMZ) and carmustine (BCNU) since these agents are commonly used in the treatment of primary and metastatic brain tumours. Chemically-engineered inhibitors of endogenous miRNAs that were significantly reduced in lung or breast cells after astrocyte co-culture (Supp. Table 1), were transfected into tumour cells and the rank order effect on growth in the presence of TMZ or BCNU determined (Fig. 3C). Many of the miRNA inhibitors enhanced cell growth even in the presence of TMZ or BCNU.

MiRNA-768-3p targets *K-ras*. Ras proteins are key regulators of signaling cascades that control proliferation, differentiation and apoptosis. Mutations in these proteins (or their effectors) are associated with pathological conditions, particularly the development of various forms of human cancer[25]. Interestingly, predictive database algorithms indicated that the *K-ras* (v-Ki-ras2 Kirsten rat sarcoma viral oncogene homolog) 3′-UTR was a direct target of miRNA-768-3p. Other miRNAs that were reduced in lung tumour cells after astrocyte co-culture were also predicted to bind the *K-ras* 3′-UTR. (Supp. Fig. 4). The seed sequence (residues 2–8) of miRNA-768-3p, which is critical for target specificity, revealed 100% homology to the *K-ras* 3′-UTR (Supp. Fig. 5). The ability of miRNA-768-3p to directly target the *K-ras* 3′-UTR was then determined using cell-based luciferase (Luc)-generated luminescent readout. A pEZ-MT01-derived clone contained the *K-ras* 3′-UTR inserted downstream of the secreted *Luc* reporter gene driven by the SV40 promoter was used to quantitate the effect of the miRNA-768-3p inhibitor or replacement. A549 cells were first transfected with pEZ-MT01-*K-ras* plasmid and then transfected with either the miRNA-768-3p inhibitor or mimic. The miRNA-768-3p inhibitor increased luminescence generated by A549 cells transfected with only the pEZ-MT01 ~ *K-ras* 3′-UTR clone relative to the scrambled control (Fig. 4A). A549 cells also transfected with the miRNA-768-3p replacement displayed reduced luminescence to indicate that increased miRNA-768-3p specifically bound to the *K-ras* 3′-UTR to reduce luminescence (Fig. 4A). We then compared the effect of miRNA reduced by co-culture (768-3p, 200c, 886-5p) with miRNAs that have reported to target *K-ras* (miRNA-141,-193b, -200a, -Let-7a and -Let-7c). A549 and H520 cells were transfected with these chemically-engineered inhibitors and the increase in growth over cells transfected with scrambled control determined (Fig. 4B). Interestingly, inhibitors of miRNA-200a and Let-7c (that target *K-ras*) both enhanced the growth of A549 and H520 cells comparable to those reduced by co-culture.

Strikingly, western blot using a pan-Ras antibody indicated that transfection of the miRNA-768-3p inhibitor increased the level of the Ras protein in A549 cells (Fig. 4C). In addition, an isoform-specific antibody indicated that the miRNA-768-3p inhibitor also increased the level of the K-ras protein. H520 cells which express wildtype (wt) *K-ras* were transfected with miRNA inhibitors, incubated for 72 h, lysates prepared and probed for K-ras levels. Transfection of the miRNA-768-3p inhibitor enhanced expressed of K-ras compared to scramble control transfected cells. The increase in K-ras was observed not only with chemically-engineered inhibitors of miRNA-768-3p but also miRNA-200c, 886-5p, 200a and Let-7c. Prior studies have demonstrated that GTP-loaded K-ras is a potent activator of the Raf-ERK pathway. As A549 cells have a G12S-oncogenic *K-ras* mutation present at both alleles, the increased expression of *K-ras* should lead to increased phosphorylation of ERK. Transfection of the miRNA-768-3p inhibitor also led to an increase in the level of CD44 and the pro-growth effectors Akt and B-Raf that function within the K-ras signaling pathway. Taken together the results suggested that miRNA768-3p inhibition increased K-ras, which in turn activated the Raf pathway[26,27].

A549 cells were transfected with clones that expressed shRNA directed against either *K-ras* or a scrambled control. Clones that expressed shRNA to reduce *K-ras* displayed reduced cell growth compared to cells that expressed the control clone (Fig. 4D). To determine whether miRNA-768-3p acted through *K-ras*, cells were first transfected with the *K-ras*-specific shRNA clones and then transfected with either the miRNA-768-3p inhibitor or scrambled (control) miRNA. Cells transfected with the scrambled clone and then transfected with the miRNA-768-3p inhibitor exhibited increased viability. However, cells transfected with clones that reduced *K-ras* did not exhibit an increase in cell viability when transfected with the miRNA-768-3p inhibitor to support the finding that miRNA-768-3p acted through *K-ras* (Fig. 4E). Finally, transfection of a chemically-engineered miRNA-768-3p replacement abolished the pro-growth effect of the miRNA-768-3p inhibitor (Fig. 4F).

Expression of miRNA-768-3p in metastatic and primary brain tumour tissue. To assess the clinical relevance of our findings, the level of miRNA-768-3p was determined in metastatic brain tissue from patients and compared to that in normal brain tissue obtained from healthy adults. The level of miRNA-768-3p was first compared in brain tissue obtained from five healthy adults relative to the control miRNA RNU6 (Fig. 5A). Next, metastatic brain tumour tissue was obtained from 19 patients diagnosed with either lung (n = 4), breast (n = 3), ovarian (n = 1), melanoma (n = 2), hepatic (n = 2), parotid (n = 1), papillary (n = 2), adenocarcinoma (primary unknown, n = 3) or large cell (n = 1) primary tumors. RT-PCR results indicated that miRNA-768-3p levels were lower in brain metastatic tissue samples than in normal brain (Fig. 5B). The level of miRNA-768-3p was slightly lower in lung and breast primary tumor tissue samples relative to expression in normal brain (Fig. 5C). Next, we compared miRNA-768-3p expression in lung primary tumor tissue to it's expression in brain metastases and saw that the expression was significantly lower in brain metastatic tissue (Fig. 5D). Finally, miRNA-768-3p was also shown to be expressed at a lower level in patient brain metastatic tissue compared to same-patient tissue from primary (lung or skin melanoma) tumour (Fig. 5E).

Discussion

Metastasis is the most significant process affecting the clinical management of cancer patients and occurs in multiple, sequential steps, however, the molecular basis underlying each step remains obscure[5]. The "seed and soil" hypothesis suggests that metastatic tumour cells exploit the brain microenvironment for their growth and survival through unique interactions[15,28]. An experimental model of the brain microenvironment using immortalized murine astrocytes was applied to study the protective effect of the brain niche by co-culture with human tumour cells. Astrocytes promoted tumour cell viability and fostered a pro-survival, chemo-protective effect on lung, breast and melanoma tumour cells. Genetic and epigenetic changes in cancer cells allow them to find the brain microenvironment a favorable niche for tumourigenic "seeds" to then grow surrounded by activated astrocytes whose physiological role is to protect neurons from toxic substances. We demonstrate that astrocytes modulate the level of individual miRNAs in tumour cells and consequently enhance tumour growth, drug resistance and the acquisition of stemness. Chemically-engineered inhibitors designed to silence individual miRNAs, similar to astrocytes, promoted cell viability, drug resistance and increased the level of K-ras. Importantly, miRNA 768-3p was reduced in metastatic brain lesions when compared to primary lung tumour from the same patient to strengthen the clinical relevance. Brain microenvironment-mediated control of miRNA expression to promote metastatic growth represents a novel, biologically and clinically relevant step in the mechanistic understanding of metastasis.

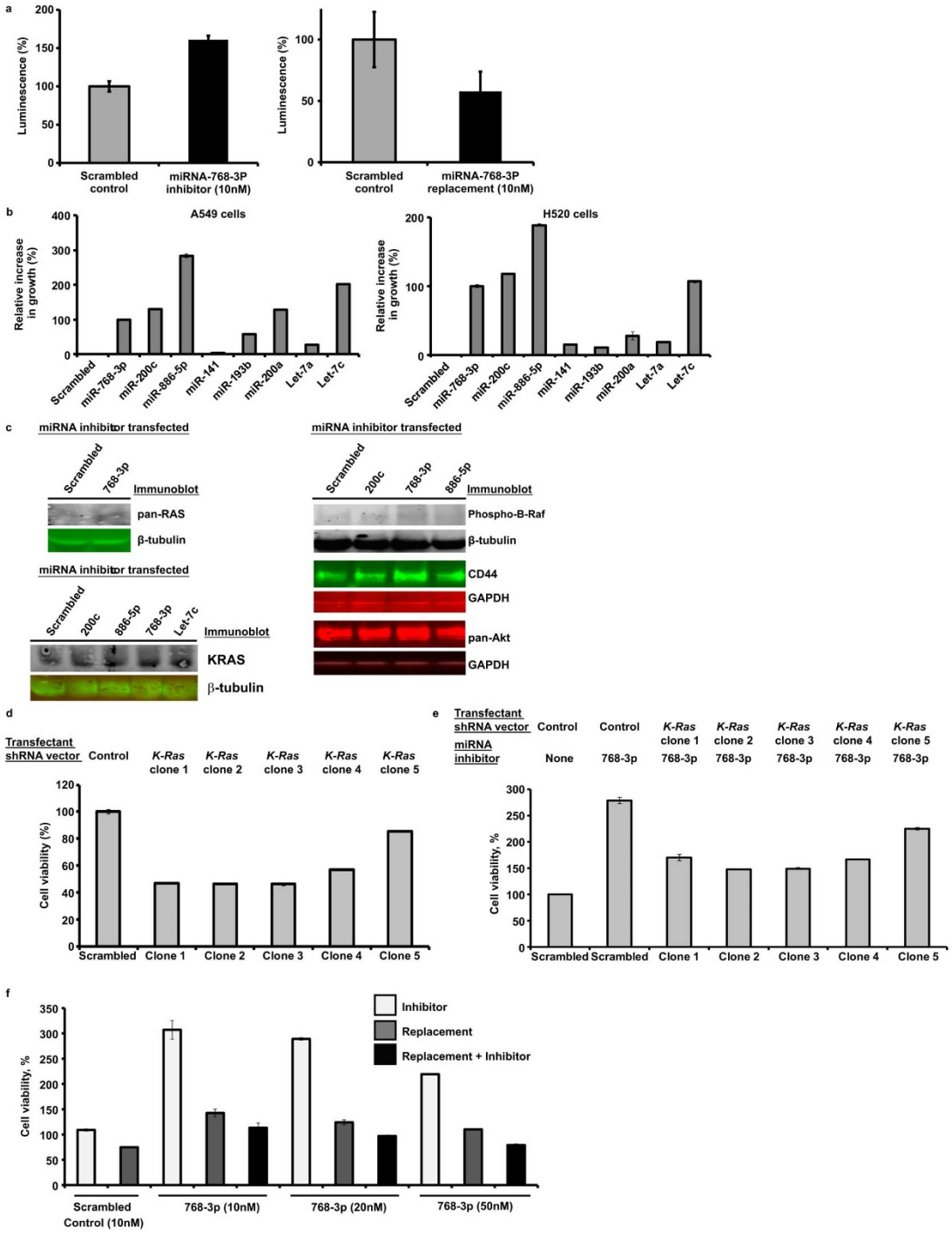

Figure 4 | miRNA-768-3p specifically targets *K-ras*. (a). Luminescent readout to determine the effect of the chemically-engineered miRNA-768-3p inhibitor or replacement on *K-ras* 3′-UTR-driven luciferase activity. (b). Effect of chemically-engineered miRNA inhibitors on viability of A549 and H520 cells. Cells were transfected with inhibitors (10 nM) designed against either scrambled control, those miRNAs reduced by co-culture or those reported to target *K-ras*. Viability was determined using the XTT assay. The average of triplicate measurements is shown and error bars represent the standard deviations. (c). Effect of miRNA inhibitors that were reduced by co-culture on the level of pan-RAS, phospho-B-Raf and CD44 and pan-Akt by western blotting. Also shown is the effect of different miRNA inhibitors on the level of K-ras in H520 cells by western blot. Cropped blots are shown and were run under the same experimental conditions. Full-length gels blots are included in the supplemental fig. 6. (d). Effect of *K-ras* shRNA-mediated knockdown on miRNA-768-3p induced cell viability. A549 cells were transfected with either control vector or vectors to knockdown *K-ras* (clones 1 through 5). Cell viability was then determined using the XTT assay. The average of triplicate measurements is shown and error bars represent the standard deviations. (e). Effect of the miRNA-768-3p replacement on cell viability after transfection with clones to knockdown *K-ras*. A549 cells were transfected with either control vector or vectors to knockdown *K-ras* (clones 1 through 5). Cells were then transfected with miRNA inhibitors (10 nM) and grown for 72 h. Cell viability was then determined using the XTT assay. The average of triplicate measurements is shown and error bars represent the standard deviations. (f). Effect of the miRNA-768-3p synthetic replacement on growth promotion by the miRNA-768-3p inhibitor. A549 cells were transfected with either scrambled control, miRNA-768-3p inhibitor, miRNA-768-3p replacement or both inhibitor and replacement at indicated concentrations. Cells were then grown for 72 h and viability was determined using the XTT assay. The average of triplicate measurements is shown and error bars represent the standard deviations.

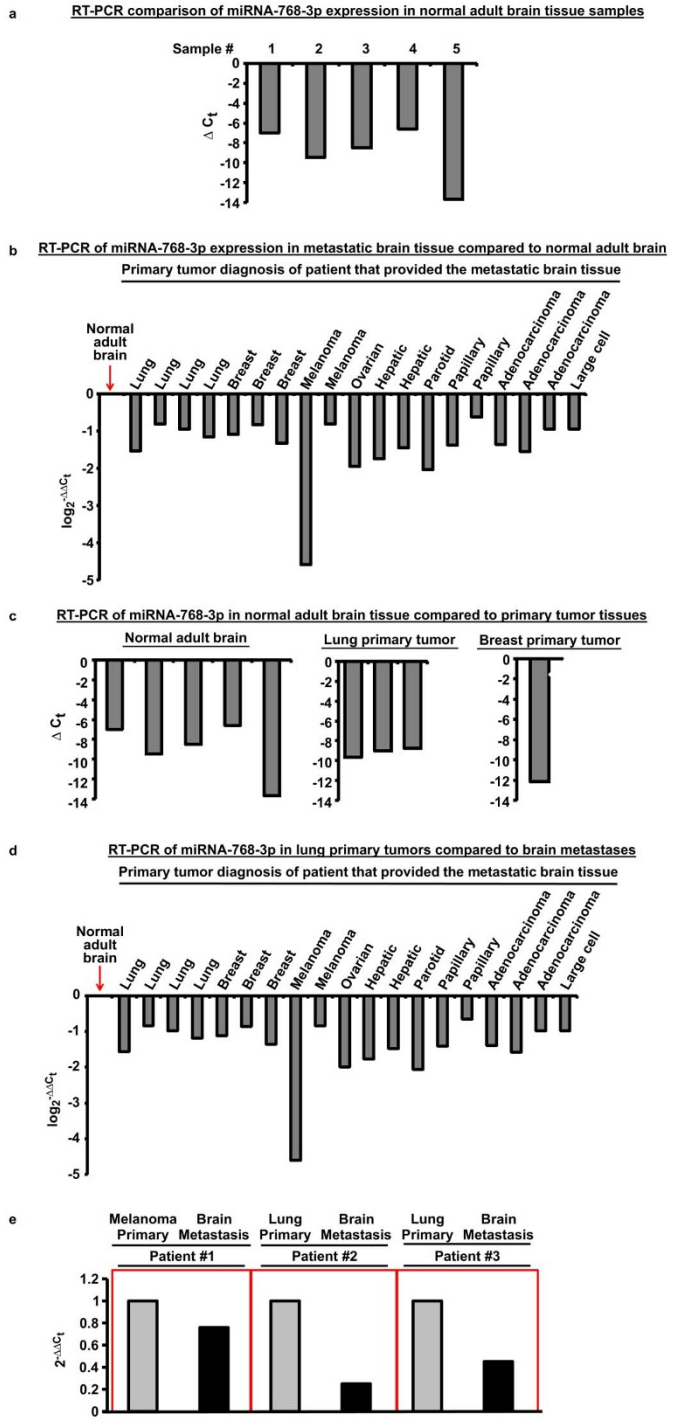

Figure 5 | Reduction of miRNA-768-3p in patient brain metastatic tissue. (a). RT-PCR was performed to determine the level of miRNA-768-3p in five different normal adult brain tissue samples relative to the control miRNA U6. (b). RT-PCR was performed to determine the level of miRNA-768-3p in brain metastatic tissue relative and normal brain to the control miRNA U6. The difference in miRNA-768-3p level relative to U6 was then normalized to 100% and converted to $\log^{2\text{-}\Delta\Delta Ct}$. Therefore, for normal brain tissue, the difference (ΔΔCt) in miRNA-768-3p from U6 expression was 100% and $\log^{2\text{-}\Delta\Delta Ct}$ was 0. The values for the difference in expression of miRNA-768-3p and U6 in each metastatic tissue specimen was then similarly determined and converted to $\log^{2\text{-}\Delta\Delta Ct}$. Shown are the $\log^{2\text{-}\Delta\Delta Ct}$ values for each metastatic tissue specimen relative to normal brain tissue. (c). Comparison of miRNA-768-3p expression in normal adult brain, lung primary tumors and breast primary tumor tissue. The level of miRNA-768-3p in five different normal adult brain tissue samples was determined relative to the control miRNA U6 and this difference was then compared to the difference on the same expression in lung primary tumor or breast primary tissue. (d). RT-PCR was performed to determine the level of miRNA-768-3p in brain metastatic tissue relative to primary lung tumor tissue using the control miRNA U6. The difference in miRNA-768-3p level relative to U6 was then normalized to 100% and converted to $\log^{2\text{-}\Delta\Delta Ct}$. Therefore, for lung primary tumor tissue, the difference (ΔΔCt) in miRNA-768-3p from U6 expression was 100% and $\log^{2\text{-}\Delta\Delta Ct}$ was 0. The values for the difference in expression of miRNA-768-3p and U6 in each metastatic tissue specimen was then similarly determined and converted to $\log^{2\text{-}\Delta\Delta Ct}$. Shown are the $\log^{2\text{-}\Delta\Delta Ct}$ values for each metastatic tissue specimen relative to normal brain tissue. (e). Quantitation of miRNA-768-3p in same-patient primary tumour and metastatic brain tissue. Human patient primary lung tumour or skin melanoma primary tumour tissue and metastatic brain tumour tissue from the same patient were analyzed by RT-PCR to determine the level of miRNA-768-3p compared to the level of U6 as was done in Fig. 5A.

A complex miRNA network functions in the regulation of tumour metastasis and miRNAs are predicted to regulate thousands of mammalian genes. However, relatively few targets have been experimentally validated and even fewer miRNA loss-of-function phenotypes have been characterized[29]. We demonstrate that one target of miR-768-3p is *K-ras*, one of the most frequently mutated oncogenes in cancers. In addition to mutational activation, Ras GTPase signaling can be upregulated by increased coupling to growth-promoting cell surface receptors. Growth factor receptors, e.g., the epidermal growth factor (EGF) family of receptor tyrosine kinases, EGFR/ErbB/HER1, ErbB2/Her2/Neu as well as Bcr-Abl, are commonly overexpressed in many cancers, causing persistent activation of Ras in the absence of *Ras* gene mutation. Thus, *Ras* activation has been shown to be an important mediator of tumour cell invasion and metastasis. The traditional view of metastasis includes a process of clonal selection in which rare variant clones within the primary tumour become capable of completing the complex, multi-step metastatic process. Additionally, using integrative genomics, *K-ras* was detected as a gene fusion with the ubiquitin-conjugating enzyme *UBE2L3* in the DU145 cell line, originally derived from prostate cancer metastasis to the brain[30]. UBE2L3-K-ras attenuates MEK/ERK signaling, commonly engaged by oncogenic mutant K-ras, and instead signals through AKT and p38 mitogen-activated protein kinase (MAPK) pathways. This was the first report of a gene fusion involving the Ras family and suggests that this aberration may drive metastatic progression in a rare subset of prostate cancers. However, the pro-survival effect of the brain microenvironment on miRNA levels within tumour cells may trigger the activation of key oncogenes, e.g., *K-ras*, indiscriminately within tumour cells and obviate the need for clonal selection or a pre-existing phenotype within the primary tumour.

Though a consensus has yet to be reached regarding the primary mechanism of miRNA action, most recent studies favor a model whereby miRNAs repress initiation of translation and facilitate target mRNA decay[31]. miRNAs are processed from much longer primary transcripts and arise from hairpin loop structures after successive enzymatic maturation steps completed by drosha and dicer in the cytoplasm. miRNAs regulate gene expression in a sequence-specific fashion and similarly, miRNA768-3p demonstrates strong homology to a region within the *K-ras* 3′ UTR. Following incorporation into the ribonucleoprotein (RNP) complex RISC (RNA-induced silencing complex, comprising proteins such as dicer and members of the argonaute (Ago) family), miRNAs bind mRNAs, primarily at their 3′ UTRs, through partial complementarity with their 'seed' sequence (the first 2 to 8 nucleotides at the 5' end of the miRNA). Consequently, mRNA translation and stability are impaired leading to a reduction in protein expression levels. Our results strongly

suggest that miRNA-768-3p binds the *K-ras* 3′ UTR leading to mRNA instability and consequently to reduce the K-ras protein level. However, it is also emerging that the effects of individual miRNAs on gene expression may be more diverse and more complex than initially proposed. Although negative regulation of gene expression occurs via mRNA cleavage and/or translational repression, studies have shown that miRNAs can also, in fact, upregulate the expression of certain target genes.

The cancer stem cell model proposes that, similar to normal tissues, cancers are also hierarchically organized and that only rare tumour cells, endowed with self-renewal and differentiation capacity (called cancer initiating cells or cancer stem cells) are capable of tumour initiation and maintenance[32–34]. In contrast, the majority of cells constituting the tumour bulk do not possess the capacity for regeneration. We demonstrate that astrocyte co-culture regulates specific miRNAs to promote CD44 expression within tumour cells and to enhance stem cell properties. Similarly, in primary GBM, stem cell features are experimentally demonstrable and CSCs are proposed to promote drug resistance. Analogous to brain metastases, the brain microenvironment may modulate miRNA within tumour cells to elicit a pro-survival phenotype. Malignant gliomas in fact have been induced in mice through the combined expression of activated forms of both K-ras and Akt in glial progenitor cells[34]. Akt activation has also been documented in GBM as a result of increased PI3-kinase activity due to mutation within the regulatory subunit of PI-3K. It is reasonable to propose that the microenvironment modulates miRNAs to foster a "CSC-like" phenotype in both metastatic and primary brain tumours.

As the number of patients who develop clinically significant brain metastasis continues to increase in the face of improving cancer therapeutics for systemic disease, there is an urgent need for the development of fully integrated clinical, basic, and translational research efforts to address this problem[5]. Current approaches to treat brain metastases include *en bloc* surgical removal, whole brain radiotherapy (WBRT), stereotactic radiosurgery (SRS), and chemotherapy. Treatment decisions must take into account clinical prognostic factors to maximize survival and neurologic function whilst avoiding unnecessary treatments. MiRNA replacement therapy aims to replenish individual miRNAs back into the tumour cells that have metastasized to the brain and re-establish a normal balance within these cells. The concept of replacing microRNAs that are lost in the disease or metastatic state has only recently been proposed[35]. The rationale for developing miRNA therapeutics is based on the premise that aberrantly expressed miRNAs play key roles in the development of human disease, and that correcting these miRNA deficiencies by either antagonizing or restoring miRNA function may provide a therapeutic benefit. Although miRNA antagonists are conceptually similar to other inhibitory therapies, restoring the function of a miRNA by replacement is a less well characterized approach. Because each miRNA targets a multitude of mRNAs involved in different signaling pathways that are often impaired in cancer, the potential of using miRNA mimics or inhibitors is a promising modality for the cancer treatment. In theory, inhibition of a particular miRNA linked to cancer onset or progression can remove the inhibition of the translation of a therapeutic protein - and conversely, administration of a miRNA mimic can boost the endogenous miRNA population repressing the translation of an oncogenic protein. Although several basic questions regarding their biological principles remain, many specific characteristics of miRNAs have triggered the exploration of employing miRNAs as potential therapeutic candidates in the treatment of brain metastases.

Methods

Cell lines. Human lung tumour (H520, A549, H661, H441) and breast (MCF-7, T47-Δ) cell lines were grown in DMEM containing 10% FBS, 1% penicillin-streptomycin and 1% glutamine.

Astrocytes co-culture. A conditionally immortalized astrocyte cell line was derived from *H-2Kb-tsA58* mice were provided through a universal biologic material transfer agreement by Dr. Isaiah Fidler, MD Anderson Cancer Center. Astrocytes were grown under permissive conditions at 33°C with a doubling time of ~ 36 h and were transfected with a GFP-expressing plasmid to facilitate separation from human solid tumour-derived cells after co-culture. Tumour cells were co-cultured with astrocytes at a ratio of ~ 2.5 : 1. Tumour cells were grown until 75% confluent, trypsinized and suspended in minimal volume of complete DMEM. Cells were then placed on top of the astrocytes and co-cultured at 37°C.

Transwell experiments. Astrocytes were grown in transwell inserts of indicated pore sizes. Tumour cells were added to the bottom chamber and allowed to further incubate with astrocytes for up to 72 h. Drugs were then added to the tumour cells and viability determined using the XTT assay.

Chemicals. Chemicals (temozolomide, paclitaxel, vincristine and bortezomib) were dissolved in DMSO or (carmustine) ethanol and obtained from Activebiochem, Maplewood, NJ.

Human tissue samples. Human tissue was obtained from the Cancer Institute Tumor Bank at the University of Cincinnati in accordance with IRB-approved protocol for human specimen collection and for the use of this material and related clinical information for research purposes. Clinical samples included paired tissue from patients that had been diagnosed with both primary lung tumours and brain metastasis. Patient tissue specimens also obtained from the UC-CITB included metastatic brain tumour tissue specimens from patients diagnosed with lung, breast, ovarian, melanoma, liver and parotid primary tumours. Metastatic brain tumor tissue was also obtained from US Biomax (Rockville, MD). Total RNA from patient primary tumors and total RNA from a third paired tumour set included the primary skin melanoma tumour and the brain metastatic tissue from the same patient and was from Biochain Institute, Inc. (Newark, CA).

Total RNA isolation. Total mRNA was isolated using the RNeasymini kit and miRNA was isolated using the miRNeasy kit (Qiagen, Valencia, CA). Total RNA was analyzed at the Cincinnati Children's Hospital Medical Center (CCHMC) Gene Expression Microarray Core. The miRNAeasy FFPE kit (Qiagen, Valencia, CA) was used to isolate RNA from human tissue samples.

FlashTag™ Biotin HSR RNA labeling Assay. The quality of total RNA was determined using an Agilent 2100 Bioanalyzer and the RNA 6000 Nano Assay. The quality control analysis confirmed the presence of low molecular weight RNA. The starting material was 1000 nanograms of total RNA and labeled using the FlashTag™ Biotin HSR RNA labeling kit. The labeled samples were then hybridized to GeneChip® miRNA 2.0 Arrays.

Vector-based forced expression. miRNArrest vector-based expression was used to specifically inhibit individual miRNAs in human tumour cells (GeneCopoeia, Rockville, MD). The vector pEZ-AMO1 expresses sequences complementary to desired miRNA target and is under control of the H1 promoter. pEZ-AMO1 also expressed an mCherry marker and puromycin selection to allow for transient suppression of target miRNAs. pEZ-AMO1 vectors which expressed either scrambled (control) or sequence to inhibit miRNA-768-3p or -5p were transfected into A549 and MCF-7 cells and grown under puromycin.

Cell Viability determination using the XTT Assay. 5×10^4 cells were plated in 250 µl of complete RPMI in a 96-well flat bottomed transparent plate, treated with drugs and incubated for 48–72 h. To determine cell viability, 50 µl of activated XTT-PMS (1 mg/ml XTT supplemented with PMS) was added to each well, plates further incubated for 4 h and absorbance determined using a BMG Labtech FLUOstar OPTIMA plate reader at 450 nm, 0.5 second position delay and 20 flashes/well.

BrDU cell proliferation. The BrdU Cell Proliferation Assay Kit (Cell Signaling Technology, Danvers, MA) detected 5-bromo-2′-deoxyuridine (BrdU) incorporated into cellular DNA during cell proliferation using an anti-BrdU antibody. Cells were cultured with labeling medium that contained BrdU into newly synthesized DNA of proliferating cells. After removing labeling medium, cells were fixed and the DNA denatured per protocol. A BrdU mouse mAb was added to detect the incorporated BrdU. Anti-mouse IgG, HRP-linked antibody was then used to recognize the bound detection antibody. HRP substrate TMB was added to develop color. The magnitude of the absorbance for the developed color was proportional to the quantity of BrdU incorporated into cells, which is a direct indication of cell proliferation.

Quantitation of sphere formation. Human solid tumour cells (A549 and MCF-7) were plated with murine astrocytes at a ratio of 2.5 : 1. No cell aggregates were present at the initiation of co-culture. Solid tumour cell spheres were then quantitated at 48 h after co-culture. Astrocytes were labeled with GFP to facilitate quantitation of tumour cells.

Determination of invasive properties. Invasion was measured using the BD biocoat matrigel invasion chamber with 8.0 mM polyethylene terephthalate membranes (BD Biosciences, Franklin Lakes, NJ). The inner well of transwell 0.8 µm inserts were coated with matrigel basement membrane matrix (1 mg/ml) and allowed to

permeabilize for 1 h. Impermeabilized liquid was removed, filters were washed with serum-free medium and allowed to air dry. Tumour cells were grown alone, with GFP^+-fibroblasts or with astrocytes for 72 h, trypsinized and $\sim 1 \times 10^6$ cells added to the inner invasion chamber in a volume of 500 µl. The outer well contained 750 µl of DMEM medium. Cells were allowed to invade for 48 h and invading cells adherent to the bottom of membrane were counted. Invading cells were enumerated by dividing membranes into quadrants and counting the number of cells in each quadrant.

Transfection of chemically-engineered miRNA inhibitors. One day prior to transfection ~ 5,000 cells were plated/well in 100 uL of media with no antibiotics. On the day of transfection the miRNA inhibitor and Endofectin Max transfection reagent (GeneCopoeia, Rockville, MD) were each diluted in 50 uL Opti-MEM (Invitrogen)/well and incubated separately at room temperature for 5 min. MiRNA and Endofectin Max were then combined and incubated at room temperature. After 30 min, 100 uL of the transfection mix was added dropwise to cells and antibiotics added 16 h post-transfection. Chemically-optimized synthetic RNA-based miRNA inhibitor or non-targeting scrambled controls (LightSwitch miRNA inhibitors, SwitchGear, Menlo Park, CA) was transfected into cells determine the effect. Inhibitors were dissolved in water and transfected into using Lipofectamine 2000 (Invitrogen, Life Technologies, Grand Island, NY) according to the manufacturer's instructions.

Transfection of miRNA replacements. Chemically-optimized, double-stranded RNA, synthetic mimics of endogenous human miRNAs, (SwitchGear, Menlo Park, CA) were transfected using Lipofectamine RNAiMax (Invitrogen, Life Technologies, Grand Island, NY).

Western blotting. A549 cells (1×10^6) in 2 ml media were plated in a 6 well plate, transfected as indicated and incubated for 48 h. Cells were trypsinized, centrifuged and supernatant discarded. Pelleted cells were suspended in 500 µl of RIPA buffer, pipetted up and down thrice, placed on ice for 5 min, centrifuged at 3000 rpm for 10 min, and 125 µl of NuPAGE® LDS sample buffer added. The sample was then incubated at 70°C for 5 min and loaded onto SuperSep™ 5–20% gradient gels (Wako Laboratory Chemicals, Richmond, VA) and separated by SDS-polyacrylamide electrophoresis[36], transferred to nitrocellulose membranes, blocked with LiCor blocking solution and probed with primary antibodies. K-ras mouse antibodies (Santa Cruz Biotechnology, F234 and Novus Biologicals, H00003845) were used used at 1 : 1000 with goat serum additive and a pan-RAS rabbit antibody (Novus Biologicals, Nb11057446) was used at 1 : 2000 dilution. ERK2 mouse (Santa Cruz, Sc1647), phospho-ERK rabbit (Cell Signaling, CS9101s), phospho-ERK rabbit (Cell Signaling, 4370), pan-Akt rabbit (Cell Signaling, 4691P), phospho-Akt rabbit (Cell Signaling, 4060P) and GADPH rabbit (Bethyl Laboratories, A300–640A) antibodies were used at 1 : 2000 dilution and CD44 mouse antibody (R&D Systems) was used at 1 : 1000. Membranes were then washed thrice with PBS containing Tween-20 (PBS-T). Li-CoR IRDye 800-CW goat anti-mouse IgG (926–32210, lot#C20510-05) and 680LT donkey (926–68023, lot# C11116-07) anti-rabbit secondary antibody added at a 1 : 2000 dilution for 60 min. Membranes were washed again thrice with PBS-T detected protein visualized using a Li-Cor Odyssey Classic image detection system with integrated software.

MicroRNA 3'-UTR target clones and luciferase-based readout. The *K-ras* 3'-UTR sequence was inserted into pEZ-MT01, a dual firefly/Renilla dual luciferase reporter mammalian expression vector (GeneCopoeia, Germantown, MD). Either the *K-ras* 3′-UTR or an empty vector (pEZ-MT01) control were then transfected into the target cells and used for functional validation of the regulatory effect of miRNA-768-3p on the *K-ras* 3′-UTR. The *K-ras* 3'-UTR sequence was obtained from public domain gene sequence databases and inserted downstream of the firefly luciferase included on miTarget 3′-UTR target clones, driven by the SV40 enhancer for expression in mammalian cells provided by GeneCopoeia (Germantown, MD). The Renilla luciferase reporter driven by a CMV promoter was cloned into the same vector (pEZX-MT01) downstream of the *K-ras* 3'-UTR and served as an internal control.

Effect of shRNA-mediated K-ras knockdown. shRNA-specific clones for the *K-ras* (v-Ki-ras2 Kirsten rat sarcoma viral oncogene human homolog) or scrambled control was from Mission shRNA (Sigma, St. Louis, MO). A549 cells were transfected with control or *K-ras* shRNA-specific clones by the lipofectamine protocol. Cells were then expanded and then transfected with either scrambled (control) or miRNA-768-3p inhibitor. Cells were grown for three days and then used for the XTT assay to determine cell viability.

1. Jemal, A. *et al.* Cancer statistics. *CA Cancer J. Clin.* **58**, 71–96 (2008).
2. Nayak, L., Lee, E. Q. & Wen, P. Y. The epidemiology of brain metastasis. *Curr. Oncol. Rep.* **14**, 48–54 (2012).
3. DiSibio, G. & French, S. W. Metastatic patterns of cancer: results from a large autopsy study. *Arch Pathol Lab Med.* **132**, 931–9 (2008).
4. Eichler, A. F. & Loeffler, J. S. Multidisciplinary management of brain metastases. *Oncologist* **12**, 884–898 (2007).
5. Maher, E. A., Mietz, J., Arteaga, C. L., DePinho, R. A. & Mohla, S. Brain metastasis: opportunities in basic and translational research. *Cancer Res.* **69**, 6015–20 (2009).
6. Sawaya, R., Bindal, R. & Lang, F. F. Metastatic Brain Tumors. in Brain Tumors. Kaye, A. H. & Laws, E. E. editors. Churchill-Livingstone, New York, NY. 999–1026 (2001).
7. Kim, S. J. *et al.* Astrocytes upregulate survival genes in tumor cells and induce protection from chemotherapy. *Neoplasia* **13**, 286–98 (2011).
8. Cordon-Cardo, C. *et al.* Expression of the multidrug resistance gene product (P-glycoprotein) in human normal and tumor tissues. *J Histochem Cytochem.* **38**, 1277–87 (1990).
9. Gupta, G. P. & Massague, J. Cancer metastasis: building a framework. *Cell* **127**, 679–95 (2006).
10. Lim, L. P. *et al.* Microarray analysis shows that some microRNAs downregulate large numbers of target mRNAs. *Nature.* **433**, 769–73 (2005).
11. Lu, J. *et al.* MicroRNA expression profiles classify human cancers. *Nature.* **435**, 834–38 (2008).
12. Nguyen, D. X. & Massague, J. Genetic determinants of cancer metastasis. *Nature Rev. Genet.* **8**, 341–52 (2007).
13. Calin, G. A. & Croce, C. M. MicroRNA signatures in human cancers. *Nat Rev Cancer.* **6**, 857–66 (2006).
14. Ma, L., Teruya-Feldstein, J. & Weinberg, R. A. Tumour invasion and metastasis initiated by microRNA-10b in breast cancer. *Nature.* **449**, 682–88 (2008).
15. Valastyan, S. *et al.* A pleiotropically acting microRNA, miR-31, inhibits breast cancer metastasis. *Cell.* **137**, 1032–46 (2009).
16. Nedergarrd, M. Direct signaling from astrocytes to neurons in cultures of mammalian brain cells. *Science* **263**, 1768–1771 (1994).
17. Langley, R. R. *et al.* Tissue-specific microvascular endothelial cell lines from H-2Kb-tsA58 mice for studies of angiogenesis and metastasis. *Cancer Res.* **63**, 2971–76 (2003).
18. Fidler, I. J. The pathogenesis of cancer metastasis: the 'seed and soil' hypothesis revisited. *Nat Rev Cancer.* **3**, 453–8 (2003).
19. Langley, R. R. *et al.* Generation of an immortalized astrocyte cell line from H-2Kb-tsA58 mice to study the role of astrocytes in brain metastasis. *Int. J. Oncol.* **35**, 665–72 (2009).
20. Berezikov, E. *et al.* Many novel mammalian microRNA candidates identified by extensive cloning and RAKE analysis. *Genome Res.* **16**, 1289–98 (2006).
21. Ono, M. *et al.* Identification of human miRNA precursors that resemble box C/D snoRNAs. *Nucleic Acids Res.* **39**, 3879–91 (2011).
22. Huttenhofer, A. *et al.* RNomics: an experimental approach that identifies 201 candidates for novel, small, non-messenger RNAs in mouse. *EMBO J.* **20**, 2943–53 (2001).
23. Li, J. H. *et al.* MicroRNA miR-886-5p inhibits apoptosis by down-regulating Bax expression in human cervical carcinoma cells. *Gynecol. Oncol.* **120**, 145–51 (2011).
24. Shimono, Y. *et al.* Downregulation of miRNA-200c links breast cancer stem cells with normal stem cells. *Cell* **138**, 592–603 (2009).
25. Downward, J. Targeting RAS signaling pathways in cancer therapy. *Nat Rev Cancer.* **3**, 11–22 (2003).
26. Davies, H. *et al.* Mutations of the BRAF gene in human cancer. *Nature.* **417**, 949–54 (2002).
27. Rajalingam, K. *et al.* Prohibitin is required for Ras-induced Raf–MEK–ERK activation and epithelial cell migration. *Nat. Cell Biol.* **7**, 837–43 (2005).
28. Paget, S. The distribution of secondary growths in cancer of the breast. *The Lancet.* **1**, 571–573 (1889).
29. Gupta, G. P. *et al.* Mediators of vascular remodeling co-opted for sequential steps in lung metastasis. *Nature* **446**, 765–70 (2007).
30. Wang, X. S. *et al.* Characterization of KRAS rearrangements in metastatic prostate cancer. *Cancer Discov.* **1**, 35–43 (2011).
31. Yates, L. A., Norbury, C. J. & Gilbert, R. J. C. The long and short of microRNA. *Cell* **153**, 516–519 (2013).
32. Gupta, P. B., Chaffer, C. L. & Weinberg, R. A. Cancer stem cells: mirage or reality? *Nat. Med.* **15**, 1010–2 (2009).
33. Singh, S. K. *et al.* Identification of a cancer stem cell in human brain tumors. *Cancer Res.* **63**, 5821–8 (2003).
34. Curtis, S. J. *et al.* Primary tumor genotype is an important determinant in identification of lung cancer propagating cells. *Cell Stem Cell* **7**, 127–33 (2010).
35. Bader, A. G., Brown, D. & Winkler, M. The promise of microRNA replacement therapy. *Cancer Res.* **70**, 7027–30 (2010).
36. Laemmli, U. K. Cleavage of structural proteins during assembly of the head of bacteriophage T4. *Nature.* **227**, 680–85 (1970).

Acknowledgements

The authors express their sincere gratitude to Dr. Isaiah J. Fidler for the immortalized murine temperature-sensitive astrocyte cell line and for insightful comments. Human tissue was obtained from the Cancer Institute Tumor Bank at the University of Cincinnati (http://cancer.uc.edu/Research/TumorBanking.aspx). JD gratefully acknowledges funding provided by the UC Brain Molecular Therapeutics Program and the Mayfield Education and Research Foundation.

Author contributions

J.D., A.T.S., R.E.W., S.L. wrote the manuscript. J.D., A.T.S. and R.E.W. were responsible for the overall experimental design. S.A., A.S. and S.J. were responsible for cell culture,

co-culture experiments, microRNA isolation, microRNA transfection, RT-PCR experiments and human tissue analysis. B.A. performed the bioinformatic analysis and K.S. and A.T.S. performed the western blotting. S.A., A.S., S.J., A.T.S. and J.D. prepared figures 1–3. A.S., S.J. and J.D. prepared figures 4 and 5. All authors reviewed the manuscript.

Additional information

Supplementary information accompanies this paper at http://www.nature.com/scientificreports

Competing financial interests: The authors declare no competing financial interests.

How to cite this article: Subramani, A. *et al*. The brain microenvironment negatively regulates miRNA-768-3p to promote *K-ras* expression and lung cancer metastasis. *Sci. Rep.* **3**, 2392; DOI:10.1038/srep02392 (2013).